



## Original Article

# Synthesis of Magnetite/Chitin/Fulvic Acid Derived from Goat Manure Compost and Adsorption Study of Zn(II) for Water Security Enhancement

Audrey Nur Aisyah<sup>1</sup>, Azzahra Sandri<sup>1</sup>, Raihansyah Raja Utama<sup>1</sup>, Mayang Fauziah Putri Kuntjahjono<sup>1</sup>, Sultan Napoleon<sup>1</sup>, Rahmat Basuki<sup>1\*</sup> 

<sup>1</sup>Department of Chemistry, The Republic of Indonesia Defense University, Kawasan IPSC Sentul, Bogor 16810, Indonesia

<https://doi.org/10.55749/ss.v1i1.79>

Received: 29 May 2025; Revised: 16 Jun 2025; Accepted: 20 Jun 2025; Published online: 30 Jun 2025; Published regularly: 30 Jun 2025  
This is an open access article under the CC BY-SA license (<https://creativecommons.org/licenses/by-sa/4.0/>).

**Abstract**— Water pollution due to heavy metals such as Zn(II) poses a risk to the environment and health. This study aims to synthesize Magnetite/Chitin/Fulvic Acid (AF)-based composite adsorbent from goat feces compost and evaluate its effectiveness in adsorbing Zn(II) ions. Fulvic acid was extracted through alkaline-acid method and synthesized together with chitin and magnetite using one pot coprecipitation method. Characterization using FTIR, XRD, and BET showed successful synthesis with mesoporous structure for BET (average pore size 6.15 nm, surface area 41.77 m<sup>2</sup>/g). Isotherm studies showed that the adsorption of Zn(II) showed a good fit with the Freundlich ( $R^2 = 0.9967$ ) and Temkin ( $R^2 = 0.9968$ ) models, indicating multilayer adsorption on the heterogeneous surface. The composite also shows good adsorption ability and can be magnetically separated, making it an environmentally friendly and efficient potential adsorbent for wastewater treatment applications.

**Keywords**— Adsorption, Fulvic acid, Goat manure compost, Magnetite/Chitin/FA, Zn(II)

## 1. INTRODUCTION

The rapid growth of industrial activities in Indonesia has led to a significant increase in wastewater discharge, much of which contains toxic substances that pose serious environmental and health risks. These contaminants can act directly, such as through acute toxicity, or indirectly through long-term interactions with soil and water ecosystems as reported by Nursabrina and colleagues in 2021. Moreover, industrial effluents contribute to the deterioration of clean water availability, potentially leading to water scarcity as projected by the World Water Forum II held in The Hague, Netherlands [1].

Heavy metals, particularly zinc ions, are among the most frequently encountered contaminants in industrial effluents. These ions commonly originate from sectors such as metal plating, battery manufacturing, and paint industries, and can be harmful to both humans and aquatic organisms when present in excessive concentrations [2]. Various treatment methods have been employed to address this issue, including adsorption, electrodialysis, ion exchange, solvent extraction, and electrocoagulation [1]. Among these, adsorption is widely preferred due to its operational

simplicity, economic feasibility, and compatibility with environmentally friendly materials [3-4].

Humic substances, particularly humic acid and fulvic acid, are naturally derived organic macromolecules known for their strong metal-binding capabilities due to the presence of acidic functional groups [5]. While humic acid has been extensively studied, fulvic acid offers superior properties such as stronger acidity, higher reactivity, and solubility across all pH conditions due to the abundance of reactive carboxyl and hydroxyl groups [6-7]. Fulvic acid extracted from goat manure compost is considered a sustainable and underutilized resource. Previous studies have demonstrated that humic substances derived from goat manure are effective in binding heavy metals from aqueous solutions [8-9].

In addition to fulvic acid, chitin is a natural biopolymer composed of N-acetylglucosamine units and is commonly obtained from the exoskeletons of marine organisms such as shrimp and crabs. Its porous structure and functional groups including amino and hydroxyl groups allow for strong interactions with metal ions through mechanisms such as complexation and ion exchange [10]. Chitin is abundant as a seafood industry

\*Corresponding author.

Email address: [rhmtbsq@gmail.com](mailto:rhmtbsq@gmail.com)

byproduct and is both biodegradable and modifiable, making it suitable for use in composite adsorbents with enhanced performance [11].

Magnetite, or iron oxide in the form of  $\text{Fe}_3\text{O}_4$ , is an inorganic material known for its high surface area and active hydroxyl groups on the surface, which provide a high affinity for metal ion adsorption [12]. Its intrinsic magnetic properties also facilitate easy separation from solution after the adsorption process using an external magnetic field, making it highly suitable for environmental applications [13].

This study aims to synthesize and characterize a composite adsorbent made from magnetite, chitin, and fulvic acid derived from goat manure compost. The composite is designed to combine the organic binding capability of fulvic acid, the structural and functional support of chitin, and the magnetic separation advantage of magnetite. Its performance in adsorbing zinc ions from aqueous solutions is evaluated through adsorption isotherms and kinetic models to determine its efficiency, selectivity, and potential for use in practical wastewater treatment applications.

## 2. EXPERIMENTAL SECTION

### 2.1. Materials

The materials used, namely goat manure compost as the main ingredient of fulvic acid extraction,  $\text{ZnSO}_4$ ,  $\text{FeCl}_3 \cdot 6\text{H}_2\text{O}$  and  $\text{FeSO}_4 \cdot 7\text{H}_2\text{O}$  produced by Merck, chitin, 1,10-phenanthroline, 0.1 M HCl solution, 0.1 M NaOH solution, and aquades.

### 2.2. Instrumentation

This research performed FTIR (Shimadzu Prestige 21), UV-Vis (Shimadzu UV-1800), SAA (Quantachrome NOVA 2200E) instrumentations. The characterization of the samples was carried out using Fourier Transform Infrared Spectroscopy (FTIR), Ultraviolet-Visible (UV-Vis) spectrophotometry, and Surface Area Analyzer (SAA). FTIR spectra were recorded using a Shimadzu Prestige 21 spectrometer within the range of  $4000\text{--}400\text{ cm}^{-1}$ , employing the KBr pellet method. Each measurement was performed with a resolution of  $4\text{ cm}^{-1}$  and 32 scans per sample. UV-Vis absorbance measurements were conducted using a Shimadzu UV-1800 spectrophotometer over the wavelength range of  $200\text{--}800\text{ nm}$ , with a quartz cuvette of 1 cm path length. The specific surface area and porosity of the samples were determined using a Quantachrome NOVA 2200E instrument based on the Brunauer–Emmett–Teller (BET) method. Prior to analysis, the samples were degassed at  $120^\circ\text{C}$  for 12 hours under vacuum, and nitrogen adsorption-desorption isotherms were recorded at 77 K.

### 2.3. Fulvic Acid Extraction

The dried and ground goat manure compost was prepared as much as 500 g and then dissolved in 5 L of 0.1 M NaOH solution and stirred at room temperature

and pressure for 24 hours. The mixture was then separated by centrifuge at 3000 rpm for 10 minutes and filtered. The filtrate obtained was acidified with 0.1 M HCl to pH 1 and later formed 2 layers, the upper layer being fulvic acid and the lower layer being humic acid. The mixture was separated by centrifuge at 5000 rpm for 15 minutes, the supernatant was taken slowly with a drop pipette (Basuki *et al.*, 2017). Humic acid solution was obtained as much as 1300 ml which was then concentrated by heating at  $40^\circ\text{C}$  until the solution became 800 ml. After concentrating fulvic acid, it was then alkalized to pH 11 by adding 0.3 g of solid NaOH.

### 2.4. Magnetite Synthesis

Magnetite ( $\text{Fe}_3\text{O}_4$ ) was synthesized using the Coprecipitation method. 4 g  $\text{FeCl}_3 \cdot 6\text{H}_2\text{O}$  and 2 g  $\text{FeSO}_4 \cdot 7\text{H}_2\text{O}$  were dissolved in 25 mL of distilled water. The mixture was heated at  $90^\circ\text{C}$  and stirred for 60 minutes. Then 25 mL of 25%  $\text{NH}_4\text{OH}$  was rapidly added and stirring and heating was continued for up to 1 hour. The mixture was then cooled for 24 hours. The resulting precipitate was filtered and washed with distilled water until the pH was neutral. Followed by drying at  $80^\circ\text{C}$  oven for 1 night to dry. The solids obtained were then characterized using FTIR, and BET instruments [14].

### 2.5. Magnetite/Chitin/AF Synthesis

Magnetite/Chitin/AF synthesis begins with the activation of chitin compounds. A total of 1.5 g chitin was activated with 100 ml acetic acid for 4 hours at  $50^\circ\text{C}$ . The activated chitin was mixed with 4 g  $\text{FeCl}_3 \cdot 6\text{H}_2\text{O}$  and 2 g  $\text{FeSO}_4 \cdot 7\text{H}_2\text{O}$  then stirred for 4 hours at a constant temperature of  $70^\circ\text{C}$ . After 4 hours, 50 ml of fulvic acid and 25 ml of ammonia were quickly mixed into the solution and stirred again for 1 hour at  $70^\circ\text{C}$ . The mixture was allowed to stand for 24 hours and rinse with distilled water until pH 7 after which it was dried with an oven at  $50^\circ\text{C}$  until completely dry.

### 2.6. Preparation of Standard Series Solution

$\text{Zn(II)}$  standard solution prepared 0.671 grams of  $\text{Zn}(\text{CH}_3\text{COO})_2$  which was then dissolved into 1000 mL of distilled water to obtain a stock solution with a concentration of 200 ppm. Furthermore, the standard solution was diluted into a 50 mL measuring flask to obtain a standard series solution with concentrations of 0, 20, 30, 40, and 60 ppm. Each volume of stock solution was taken as much as 5; 7.5; 10; and 60 mL. Then distilled water was added until it reached the final volume. Each standard solution was then dripped with 1,10-phenanthroline solution as a complexation indicator, followed by analysis using a UV-VIS spectrophotometer.

### 2.7. Non-competitive Adsorption Isotherm

A total of 50 mg of sample was interacted with 30 mL of  $\text{Zn(II)}$  metal ion solution with various concentrations of 30, 40, 50, 60, 70, 100 ppm for 3 hours. The filtrate of

each mixture was then taken. The concentration of metal ions after adsorption was analyzed by UV-Vis Spectrophotometer.

## 2.8. Non-competitive Adsorption Kinetics

A total of 50 mg of sample was interacted with 50 mL of 50 ppm Zn(II) metal ion solution at optimum pH. This mixture was then stirred with a time variation of 5, 10, 20, 30, 50, 60, and 120 minutes. After fulfilling the specified time limit, the filtrate of each mixture was taken. The adsorbate concentration after adsorption was analyzed by UV-Vis Spectrophotometer.

## 3. RESULT AND DISCUSSION

### 3.1. Fulvic Acid Extraction

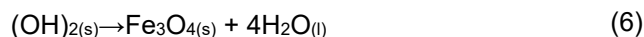
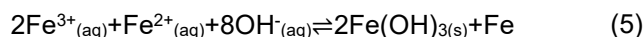
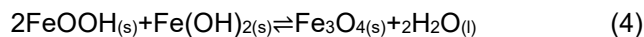
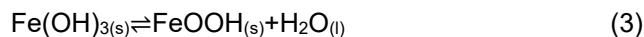
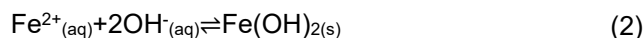
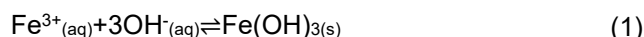
Fulvic acid is a natural organic compound formed from the decomposition of organic matter in the soil and plays a role in the formation of humus or humic compounds [15]. Unlike humic acid which is insoluble at pH below 3, fulvic acid is soluble at various pH [7]. In this study, fulvic acid was extracted from goat feces compost that had undergone a 7-month composting process at a farm in Tegal, Central Java. The compost was dried and pulverized first to facilitate the extraction process. Extraction was done by soaking the compost in NaOH solution, then adding HCl. The use of NaOH aims to hydrolyze complex compounds such as humic acid, lignin, and polysaccharides so that fulvic acid can dissolve in water, and separate insoluble compounds [16]. The addition of HCl is done to lower the pH, precipitate humic acid, remove residual bases, and neutralize the solution. This process produces two layers, the top layer is a clear brown solution (fulvic acid) and the bottom layer is dark brown solids (humic acid) [1].

The solution in the form of fulvic acid is continued to be extracted by concentrating and increasing the pH value until it reaches pH 11. The concentration of fulvic acid aims to increase its concentration, so as to strengthen chemical interactions with metal ions or other compounds, and increase efficiency in processes such as adsorption and complex formation. Increasing pH is also done to increase solubility, reactivity, and effective interaction with metal ions or other compounds [17]. Setting the pH also helps neutralize the influence of too strong acids or bases, supports system stability, and maximizes the performance of fulvic acid. Fulvic acid that has been extracted from goat feces compost.

### 3.2. Magnetite/Chitin/AF Composite Synthesis

Magnetite/Chitin/AF composite synthesis was carried out using the onepot hydrothermal coprecipitation synthesis method, where activated chitin was reacted with  $\text{Fe}^{2+}$ ,  $\text{Fe}^{3+}$  and  $\text{NH}_4\text{OH}$  ions as well as Fulvic Acid (AF) rapidly at high temperature. After being reacted simultaneously for 6 hours and allowed to stand for 24 hours the composite will be formed. The following

reaction is proposed for the formation mechanism of  $\text{Fe}_3\text{O}_4$  [18]. In this process, precipitated ferric and ferric hydroxides react with hydroxide ions ( $\text{OH}^-$ ) to form ferric and ferrous hydroxides (Equation 1) and ferrous hydroxides (Equation 2), respectively.



In the second stage, ferric hydroxide will undergo decomposition and turn into  $\text{FeOOH}$  according to Equation (3). This decomposition process occurs due to certain changes in conditions that cause ferric hydroxide to break down into a more stable compound,  $\text{FeOOH}$ . Furthermore, in a follow-up reaction, there is a solid interaction between  $\text{FeOOH}$  and  $\text{Fe}(\text{OH})_2$ , which results in the formation of magnetite and water, as described in Equation (4). This reaction is an important part of the magnetite synthesis process, where the product formed is magnetite. The overall reaction that describes the entire magnetite synthesis process can be found in Equation (5) [18].

After magnetite is formed, which is marked by a change in color to black after adding  $\text{NH}_4\text{OH}$ , chitin and fulvic acid then interact with the magnetite surface through a chemical process involving functional groups present in each of these compounds [19]. Chitin, which is a natural polymer consisting of glucosamine units containing hydroxyl ( $-\text{OH}$ ) and amide ( $-\text{NH}$ ) groups, has the ability to bind with magnetite [20]. These bonds can form through hydrogen interactions or coordination bonds involving Fe ions on the magnetite surface. These interactions give Magnetite/Chitin composites special properties that can improve their functional characteristics [21]. Fulvic acid, which is rich in carboxylic groups ( $-\text{COOH}$ ), has the ability to bind with Fe ions on the magnetite surface through a ligand exchange process [22]. In this process, the carboxylic groups present in fulvic acid will interact with Fe ions on the magnetite surface, forming a stable bond. This process enriches the Magnetite/Chitin/Fulvic Acid (AF) composite with new properties that can improve its performance in various applications, such as in heavy metal sorption processes.

The synthesized Magnetite/Chitin/AF composite has a smooth solid shape with a brownish color and has strong magnetic properties when attracted by an external magnet. This composite will be further analyzed through the characterization of existing functional groups, namely using FTIR (Fourier Transform Infrared Spectroscopy) and XRD (X-ray Diffraction) techniques and for the specific surface area (SBET) of Magnetite/Chitin/AF will be analyzed using the BET (Brunauer-Emmett-Teller) method. The FTIR technique

itself will provide information about the chemical bonds formed between chitin, fulvic acid, and magnetite through observations on the infrared spectrum. Likewise, the BET method will help determine the specific surface area of the successfully synthesized Magnetite/Chitin/AF composite. Thus, the successful synthesis and characterization of this composite will be scientifically proven and provide further insight into the potential applications of this material.

### 3.3. Functional Group Analysis

The synthesized Magnetite/Chitin/AF composite was then analyzed using FTIR spectroscopy to confirm the success of the formation process, through the detection of functional groups typical of magnetite, chitin, and fulvic acid through observation of the infrared spectrum. In this study, FTIR analysis was carried out in the absorption frequency range between 400 to 4000  $\text{cm}^{-1}$ , which made it possible to identify the functional groups in the Magnetite/Chitin/AF composite. Each functional group has a different vibration frequency, resulting in a unique spectrum and can be used to distinguish and confirm the presence of these components [18]. **Figure 1** displays the FTIR spectra for magnetite, chitin, fulvic acid and magnetite/chitin/AF materials showing the functional groups formed.

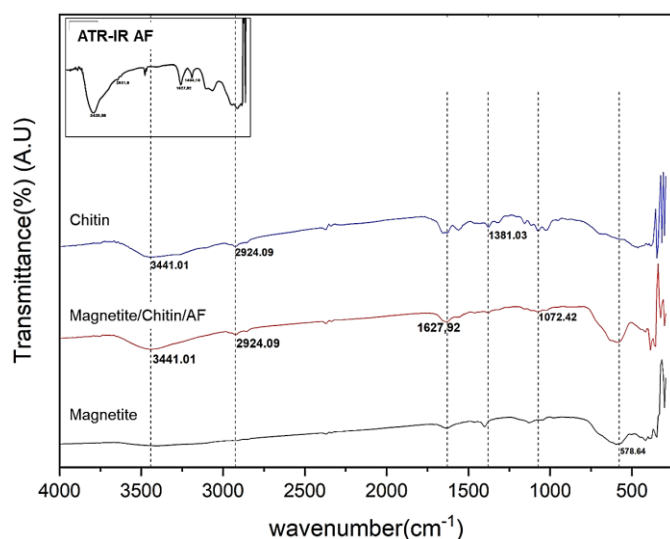


**Figure 1.** Functional groups characterization of magnetite, magnetite/chitin/af, chitin, fulvic acid

Fulvic acid successfully extracted from goat feces compost was confirmed by the presence of typical peaks of humic compounds as described by Stevenson (1944) [23], namely -COOH and -OH groups. In this study, fulvic acid analysis was carried out using the ATR technique because the fulvic acid used was in the form of a solution. **Figure 1** show the absorption of the -OH group at the peak of 3425  $\text{cm}^{-1}$ , the absorption of the aliphatic C-H group at the peak of 2932  $\text{cm}^{-1}$ , as well as the absorption of the aromatic C=C group conjugated with other double bonds, and the absorption of the C=O group contained in the carboxylate at the peak of 1628  $\text{cm}^{-1}$  and 1404  $\text{cm}^{-1}$  indicating the deformation of the

aliphatic C-H group. The results of fulvic acid analysis in this study are in accordance with Stevenson (1994) in Basuki *et al.* [1] which is characterized by the appearance of typical peaks of humic compounds at wave numbers 3400  $\text{cm}^{-1}$ , 2900  $\text{cm}^{-1}$ , and 1600  $\text{cm}^{-1}$ . The results of this study also confirmed the same as those reported by Krisbiantoro *et al.* [19]. Fulvic acid from peat soil of Rawa Pening, Ambarawa has an absorption peak at 3410  $\text{cm}^{-1}$  which is the stretching vibration of the -OH group. Peak 2931  $\text{cm}^{-1}$  is C-H aliphatic. The 1635  $\text{cm}^{-1}$  peak is an aromatic C=C conjugated with another double bond and C=O in carboxylate.

**Figure 1** also confirms the synthesis of Magnetite/Chitin/AF by the presence of vibrational absorption of characteristic groups of fulvic acid, magnetite, and chitin. There are typical fulvic acid peaks in the FTIR spectrum, namely 3441  $\text{cm}^{-1}$  (-OH), 2924  $\text{cm}^{-1}$  (-C-H stretching), and 1628  $\text{cm}^{-1}$  which indicates the presence of carbonyl groups (C=O) from carboxyl groups (-COOH). The peak at 1072  $\text{cm}^{-1}$  is associated with C-O stretching vibrations in the -COOH group. Meanwhile, the FTIR spectrum of chitin showed a characteristic peak at 3441  $\text{cm}^{-1}$  reflecting the stretching vibration of hydroxyl group (-OH). In addition, an acyl group ( $\text{CH}_3\text{C}=\text{O}$ ) was identified at 1381  $\text{cm}^{-1}$  which is related to C=O stretching vibrations and C- $\text{CH}_3$  asymmetric bending. Then there are also absorption peaks at 1628  $\text{cm}^{-1}$  and 1566  $\text{cm}^{-1}$  which are C=O (amide I) stretching vibrations and N-H (amide II) bending vibrations, which indicate the presence of amide groups in the chitin structure. The existence of a bond between the nitrogen atom in the amide group (NH) and the carbon atom of the acyl group ( $\text{CH}_3\text{C}=\text{O}$ ) was also confirmed at 1566  $\text{cm}^{-1}$  through N-C amide stretch vibrations Gunzler and Gremlich [24].

The presence of  $\text{Fe}_3\text{O}_4$  is confirmed through the detection of an absorption band at 579  $\text{cm}^{-1}$  which shows the Fe-O stretching vibrations typical of magnetite (**Figure 1**) where after synthesizing it is seen in Magnetite/Chitin/AF that the peak becomes sharper [25]. The presence of chitin in the formed Magnetite/Chitin/AF material is thought to have interacted with the -OH and -NH groups of chitin [26]. Although all chitin peak bands remained detected in the FTIR spectrum, some experienced significant shift changes. After magnetite was integrated into chitin, the frequency of hydroxyl and C-H stretching groups which initially appeared at 3425  $\text{cm}^{-1}$  and 2932  $\text{cm}^{-1}$  shifted to 3441  $\text{cm}^{-1}$  and 2924  $\text{cm}^{-1}$  in Magnetite/Chitin/AF, in addition to the vibrations at the peak of the acyl group ( $\text{CH}_3\text{C}=\text{O}$ ) 1381  $\text{cm}^{-1}$  in chitin experienced band widening after becoming a composite. This shift indicates the interaction between Magnetite, chitin, and fulvic acid [18].

### 3.4. Adsorption Analysis of $\text{N}_2$ Gas

The surface area of the Magnetite/Chitin/AF adsorbent can be analyzed by the  $\text{N}_2$  gas adsorption method with the Brunauer-Emmett-Teller (BET) equation, the results of



which can be seen in **Figure 2** and **Table 1**. Based on **Figure 2**, the isotherm pattern obtained from the isotherm analysis is in accordance with the type IV isotherm according to the IUPAC classification [18].

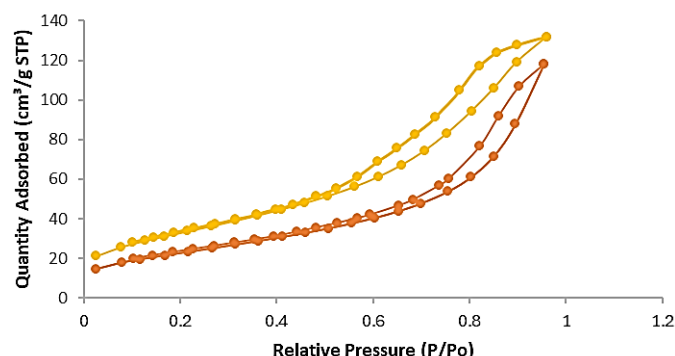


**Figure 2.** Nitrogen adsorption-desorption isotherms of magnetite/chitin/af and magnetite

This is characterized by the presence of H-1 type hysteresis loop [18]. This type IV isotherm reflects that the analyzed material has a porous structure with pore sizes ranging from 15 to 1000 Å (1.5 to 100 nm), where the inflection point (knee) on the adsorption curve generally appears when almost the entire surface of the solid has been coated by the first layer of nitrogen gas (Kusuma *et al.*, 2017). This isotherm pattern also shows typical characteristics of porous materials with mesoporous structures [27]. Based on the data presented in **Table 1**, the pore size distribution of Magnetite and Magnetite/Chitin/AF materials is dominated by pore diameters of 5.6101 nm and 6.1524 nm. Considering that the pore size range between 2 to 50 nm is categorized as mesopores [28], this material can be classified as a mesoporous material. The existence of this mesoporous structure provides an advantage in adsorption applications, due to the relatively large surface area and pore structure that supports a more optimal molecular diffusion process [18].

**Table 1.** N<sub>2</sub> gas adsorption isotherm analysis results

Adsorbent	S <sub>BET</sub> (m <sup>2</sup> /g)	V <sub>Total</sub> (cm <sup>3</sup> /g)	Average pore size (nm)
Magnetite	52.0954	0.200281	5.6101
M/Chitin/AF	41.7681	0.130629	6.1524

Based on the data in **Table 1**, the SBET value is 41.7681 m<sup>2</sup>/g, while the pore volume based on the Barrett-Joyner-Halenda (BJH) method is recorded as 0.130629 cm<sup>3</sup>/g with an average pore diameter of 6.1524 nm. Although the BJH method tends to give smaller estimates for mesoporous materials (<10 nm), this approach remains the standard in the characterization of porous materials (Khusnood *et al.*, 2024). In **Table 1**, it can be seen that the specific surface area of Magnetite/Chitin/AF (41.7681 m<sup>2</sup>/g) is lower when compared to the surface area of compound Magnetite (52.0954 m<sup>2</sup>/g). This lower surface area indicates that the composite modification of Magnetite with chitin and active components from AF caused a decrease in the number of available active sites. Research by

Pylypchul *et al.* [29] also supports this statement, where magnetite material that has been modified with chitosan has a smaller surface area compared to pure magnetite material.

### 3.5. Metal Ion Complexation

The evaluation of the adsorbent's performance in removing Zn(II) ions was initiated by determining the maximum wavelength using UV-Vis spectrophotometry. Zn(II) ions exhibited a maximum absorption wavelength at 519 nm. The absorbance data obtained at this wavelength were used for further quantitative analysis. A calibration curve was constructed using Zn(II) standard solutions with concentrations of 6, 10, 14, 18, and 22 ppm. The resulting linear regression showed a correlation coefficient ( $R^2$ ) of 0.9952, indicating a strong linear relationship between concentration and absorbance (**Figure 3**). This regression equation was subsequently used as a quantitative reference to determine the concentration of Zn(II) ions in the samples after the adsorption process using the Magnetite/Chitin/AF composite material.

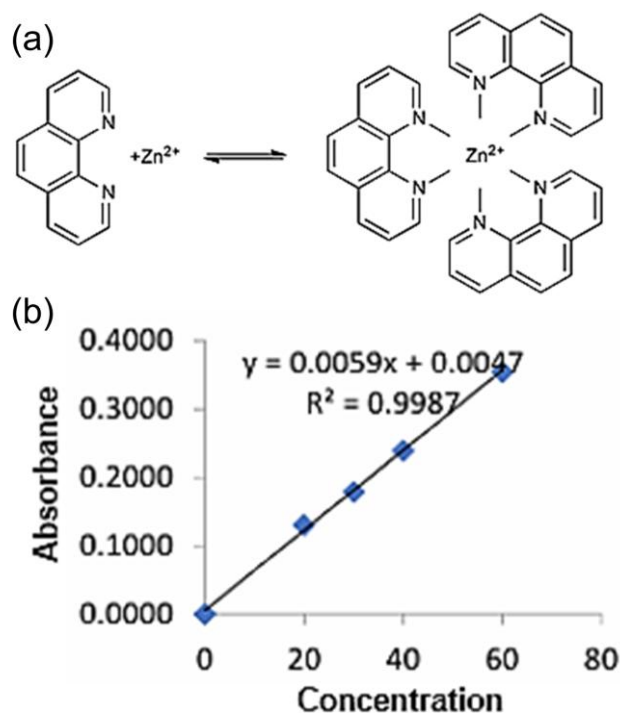


**Figure 3.** (a) Complexation reaction of Zn-metal with phenanthroline (Zn-Phenanthroline); (b) Standard curve for Zn-Phenanthroline.

### 3.6. Isotherm Analysis

The adsorption capacity of Zn(II) ions onto the Magnetite/Chitin/AF composite was evaluated using several adsorption isotherm models, including Langmuir (by plotting  $C_e/q_e$  versus  $C_e$ ), Freundlich (by plotting  $\ln q_e$  versus  $\ln C_e$ ), Dubinin–Radushkevich (D–R) (by plotting  $\ln q_e$  versus  $\epsilon^2$ ), and Temkin (by plotting  $q_e$  versus  $\ln C_e$ ).

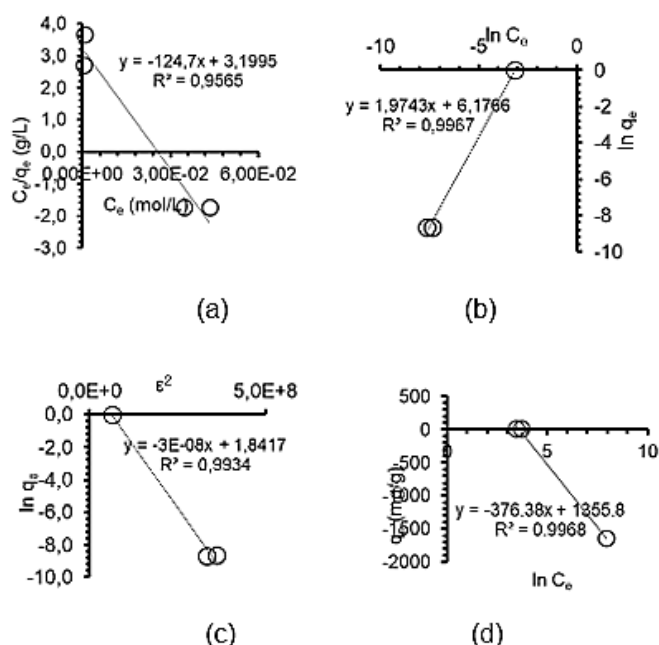


**Figure 4.** Isotherm model plots for Zn(II) adsorption onto Magnetite/Chitin/AF composite: (a) Langmuir, (b) Freundlich, (c) Dubinin–Radushkevich, and (d) Temkin.

As shown in **Figure 4**, the Freundlich isotherm model (Fig. 4b) provided the best fit for the Zn(II) adsorption process, with a correlation coefficient ( $R^2$ ) of 0.9967 (**Table 2**). This value is higher than those obtained from the other isotherm models, indicating that Zn(II) adsorption occurs predominantly via a multilayer mechanism on a heterogeneous adsorbent surface [18]. The multilayer adsorption is likely attributed to the presence of various functional groups such as carboxylic ( $-\text{COOH}$ ), phenolic ( $-\text{OH}$ ), and other active sites, where the strongest interactions occur in the initial adsorption layer, followed by subsequent layers with lower adsorption energies [30]. Based on the Freundlich model, the multilayer adsorption capacity of Zn(II) on the Magnetite/Chitin/AF composite was determined to be 409.2643 mg/g. The adsorption energy of Zn(II) was calculated to be 23.288 kJ/mol, which greatly exceeds the typical ranges for physisorption ( $<8$  kJ/mol) and ion exchange (8–16 kJ/mol) [18]. This high energy value strongly indicates that the adsorption process is governed by chemisorption, involving the formation of specific chemical bonds between Zn(II) ions and the active functional groups present on the surface of the Mag/Ch/FA composite.

The Dubinin–adushkevich (DR) isotherm analysis for Zn(II) adsorption on the Magnetite/Chitin/Fulvic Acid (Mag/Ch/FA) composite yielded a high correlation coefficient ( $R^2 = 0.9934$ ), indicating a strong agreement between the experimental data and the DR model. This suggests that the adsorption process for Zn(II) occurs predominantly through a multilayer mechanism, consistent with the theoretical basis of the DR model, which accounts for potential pore-filling phenomena and interactions beyond monolayer coverage [31]. These

findings are further corroborated by the Freundlich isotherm, which similarly assumes heterogeneous surface adsorption and supports the multilayer behavior observed in this system.

**Table 2.** Adsorption isotherm parameters for Zn(II) ions

Isotherm Parameters	Value (for $\text{Zn}^{2+}$ )
<u>Langmuir</u>	
$b$ (mg/g)	117.844
$E_L$ (kJ/mol)	23.288
$R^2$	0.9565
<u>Freundlich</u>	
$B$ (mg/g)	409.2643
$n$	0.5065
$R^2$	0.9967
<u>DR</u>	
$q_{DR}$ (mg/g)	1162.19
$R^2$	0.9934
<u>Temkin</u>	
$b_T$ (J/mol)	115.375
$A_T$ (L/g)	1.2601
$R^2$	0.9968

Additionally, the adsorption of Zn(II) ions was found to conform well to the Temkin isotherm model, as reflected by a high  $R^2$  value of 0.9968 and an adsorption energy ( $b_T$ ) of 115.375 J  $\text{mol}^{-1}$ . The Temkin model assumes a linear decrease in adsorption energy as surface coverage increases, due to adsorbate–adsorbate interactions that influence adsorption heat distribution [30]. Furthermore, the model posits a uniform distribution of binding energies up to a certain maximum, indicative of a progressive saturation of active sites on the adsorbent surface [32]. In multilayer adsorption systems, the  $b_T$  parameter can be interpreted as the average energy associated with Zn(II) ions at the outermost adsorption layer interacting with the surface of the Mag/Ch/FA composite [18].

**Table 3.** Comparison of magnetite-based adsorption capacity for Zn(II) as adsorbate

Adsorbent	$b$ (mg/g)	References
M/Chitin/AF	409.26	This research
Carboxymethylchitosan Nanoparticles	131.00	[33]
EDTA-modified magnetic chitosan nanocomposite	32.89	[34]
Magnetite-Baobab	37.04	[35]

The Magnetite/Chitin/FA composite used in this study demonstrated excellent adsorption performance, particularly for Zn(II) ions, with a significantly higher adsorption capacity compared to previously reported materials (**Table 3**). This indicates the strong potential of Mag/Ch/FA for application in the remediation of heavy metal-contaminated water. The superior performance can be attributed to the abundance of active functional groups, such as carboxyl ( $-\text{COO}^-$ ) and phenolic groups, which play a critical role in metal ion binding. Overall,

the Mag/Ch/FA composite offers a promising, environmentally friendly, renewable, and readily available adsorbent material that can be easily separated from aqueous media using an external magnetic field, eliminating the need for additional post-treatment steps.

### 3.7. Kinetics Analysis

Studies on chemical kinetics play a crucial role in understanding the adsorption rate and the factors influencing it. In this study, the adsorption kinetics of Zn(II) ions onto the Magnetite/Chitin/Fulvic Acid composite were analyzed using several commonly applied kinetic models, including the pseudo-first-order model by Lagergren and the pseudo-second-order model by Ho.

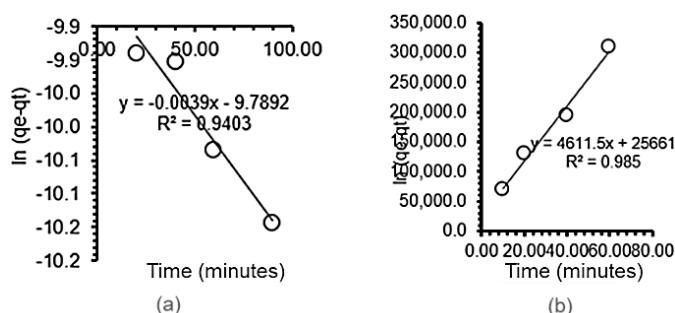


**Figure 5.** Kinetic model plots for Zn(II) adsorption onto the Mag/Ch/FA: (a) Lagergren pseudo-first-order model and (b) Ho pseudo-second-order model

The adsorption rate of Zn(II) ions onto the Magnetite/Chitin/Fulvic Acid (Mag/Ch/FA) composite was analyzed over a contact time range of 20 to 120 minutes, as illustrated in **Figure 5**. The Lagergren pseudo-first-order model suggested that rapid physical adsorption dominated the initial stage of the process. In contrast, the Ho pseudo-second-order kinetic model indicated that chemisorption was the main mechanism controlling the adsorption rate over longer time intervals [36].

**Table 4.** Adsorption kinetics parameters for Zn(II) ions

Kinetics Parameters	Value (for Zn <sup>2+</sup> )
<b>Lagergren</b>	
Calc. $q_e$ ( $\times 10^{-5}$ mol/g)	$7.927 \times 10^2$
$k_{Lag}$ (min <sup>-1</sup> )	3465.9
$R^2$	0.9473
<b>Ho</b>	
Calc. $q_e$ ( $\times 10^{-5}$ mol/g)	$2.168 \times 10^2$
$K_{Ho}$ (g min <sup>-1</sup> min <sup>-1</sup> )	828.7257
$R^2$	0.9850

According to the data presented in **Table 4**, the Ho model yielded the highest correlation coefficient ( $R^2$ ), closest to unity, indicating a better fit with the experimental data. Furthermore, the calculated equilibrium adsorption capacity ( $q_e$ ) from the Ho model was in closer agreement with the experimentally observed values listed in **Table 4**. This suggests that the adsorption of Zn(II) ions follows the pseudo-second-

order kinetics, implying that the process is governed by chemisorption, involving ionic interactions (electrostatic attraction) between negatively charged functional groups on the adsorbent surface and the positively charged Zn(II) ions [18]. Overall, the kinetic behavior of Zn(II) adsorption on Mag/Ch/FA is best described by the Ho pseudo-second-order model.

## 4. CONCLUSION

The synthesis of Magnetite/Chitin/AF has been successfully carried out by the one pot hydrothermal coprecipitation method, this is indicated by the formation of Magnetite/Chitin/AF composite solids which have been confirmed by analysis using FTIR. The results of the analysis with FTIR showed the presence of typical groups of Magnetite, Chitin, and fulvic acid compounds in the sample. Zn(II) adsorption is more in line with the Freundlich model ( $R^2 = 0.9967$ ), indicating a multilayer process on the heterogeneous surface, with a capacity of 409.2643 mg/g. The high adsorption energy ( $>20$  kJ/mol) indicates a chemisorption mechanism.

## SUPPROTING INFORMATION

There is no supporting information in this paper. The data supporting this research's findings are available on request from the corresponding author (R.Basuki).

## ACKNOWLEDGEMENT

The authors sincerely acknowledge the financial support provided by the Department of Chemistry, Republic of Indonesia Defense University. The authors also extend their gratitude for the facilities and laboratory resources made available by the BRIN.

## CONFLICT OF INTEREST

There was no conflict of interest in this study.

## AUTHOR CONTRIBUTIONS

ANA performed the conceptualization, investigation, methodology, RB supervises the experiment, data calculation, and revise the manuscript. MFPK, SN, AS, and RRH collaborated on writing and revising the manuscript. All authors approved the final version of the manuscript.

## REFERENCES

- [1] Basuki, R., Santosa, S.J., & Rusdiarso, B. 2017. Ekstraksi adsorben ramah lingkungan dari matriks biologi: asam humat tinja kuda (AH-TK). *Chempublish Journal*. 2(1). 13-25.
- [2] Wathoni, A.Z., Pratiwi, A.I., & Suci, F.C. 2021. Penurunan kadar logam berat nikel limbah cair industri pada pengolahan air limbah industri di karawang. *Journal of Industrial Process and Chemical Engineering (JOICHE)*. 1(2). 40-45. Doi: <https://doi.org/10.31284/j.joiche.2021.v1i2.2440>
- [3] Widayatno, T. 2017. Adsorpsi logam berat (Pb) dari limbah cair dengan adsorben arang bambu aktif. *Jurnal teknologi bahan alam*. 1(1). 17-23.
- [4] Nurdila, F.A., Asri, N.S. & Suharyadi, E. 2015. Adsorpsi logam Tembaga (Cu), Besi (Fe), dan Nikel (Ni) dalam limbah cair buatan menggunakan nanopartikel cobalt ferrite (CoFe<sub>2</sub>O<sub>4</sub>)



- Jurnal Fisika Indonesia*. 19(55). 23-27. Doi: <https://doi.org/10.22146/jfi.24368>
- [5] Ngatijo, N., Bemis, R., & Ihsan, M. 2021. Nanofikasi fraksi tanah gambut untuk modifikator nanomagnetit/ah-kitosan sebagai kandidat penanggulangan pencemaran zat warna. *Chempublish Journal*. 5(2). 140-150. Doi: <https://doi.org/10.22437/chp.v5i2.11105>
  - [6] Ukalska-Jaruga, A., Bejger, R., Debaene, G. & Smreczak, B. 2021. Characterization of soil organic matter individual fractions (fulvic acids, humic acids, and humins) by spectroscopic and electrochemical techniques in agricultural soils. *Agronomy*. 11(6). 1067. Doi: <https://doi.org/10.3390/agronomy11061067>
  - [7] Zhang, Y., Qin, X., An, J. & Zu, B. 2025. Adsorption and reduction of Cr(VI): mechanistic investigations of magnetite-fulvic acid complexes. *Environ. Technol.* 1-13. Doi: <https://doi.org/10.1080/09593330.2025.2546122>
  - [8] Hidayah, M., Kustomo, K., & Yunita, A.N.I. 2022. Batch adsorption of Pb(II) batch using humic acid from goat dung. *Al Kimiya: Jurnal Ilmu Kimia dan Terapan*. 9(2). 55-61. <https://doi.org/10.15575/ak.v9i2.19735>
  - [9] Luo, S., Zhen, Z., Zhu, X., Ren, L., Wu, W., Zhang, W., Chen, Y., Zhang, D., Song, Z., Lin, Z. and Liang, Y.Q. 2021. Accelerated atrazine degradation and altered metabolic pathways in goat manure assisted soil bioremediation. *Ecotoxicol. Environ. Saf.* 221. 112432. Doi: <https://doi.org/10.1016/j.ecoenv.2021.112432>
  - [10] Shahib, I.I., Ifthikar, J., Wang, S., Elkhilfi, Z., He, L. & Chen, Z., 2023. Elimination of hazardous Se(IV) through adsorption-coupled reduction by iron nanoparticles embedded on mesopores of chitin obtained from waste shrimp shells. *Environmental Science and Pollution Research*. 30(57). 119961-119973. Doi: <https://doi.org/10.1007/s11356-023-30743-x>
  - [11] Rahaman, M.H., Islam, M.A., Islam, M.M., Rahman, M.A., & Alam, S.N. 2021. Biodegradable composite adsorbent of modified cellulose and chitosan to remove heavy metal ions from aqueous solution. *Current Research in Green and Sustainable Chemistry*. 4. 100119. <https://doi.org/10.1016/j.crgsc.2021.100119>
  - [12] Shi, J., Li, H., Lu, H., & Zhao, X. 2015. Use of carboxyl functional magnetite nanoparticles as potential sorbents for the removal of heavy metal ions from aqueous solution. *J. Chem. Eng. Data*. 60(7). 2035-2041. Doi: <https://doi.org/10.1021/je5011196>
  - [13] Amjadi, M., Samadi, A., & Manzoori, J.L. 2015. A composite prepared from halloysite nanotubes and magnetite (Fe<sub>3</sub>O<sub>4</sub>) as a new magnetic sorbent for the preconcentration of cadmium (II) prior to its determination by flame atomic absorption spectrometry. *Mikrochim. Acta*. 182. 1627-1633. Doi: <https://doi.org/10.1007/s00604-015-1491-y>
  - [14] Ngatijo, Marlinda, L., Malikah, W., Ishartono, B., & Basuki, R. 2023. Magnetically separable humic acid-chitin based adsorbent as Pb(II) uptake in synthetic wastewater. *Indones. J. Chem. Stud.* 2(1). 13-21. Doi: <https://doi.org/10.55749/ijs.v2i1.22>
  - [15] Zhang, P., Zhang, H., Wu, G., Chen, X., Gruda, N., Li, X., Dong, J. & Duan, Z. 2021. Dose-dependent application of straw-derived fulvic acid on yield and quality of tomato plants grown in a greenhouse. *Front. Plant Sci.* 12. 736613. Doi: <https://doi.org/10.3389/fpls.2021.736613>
  - [16] Zavarzina, A.G., Danchenko, N.N., Demin, V.V., Artemyeva, Z.S. and Kogut, B.M. 2021. Humic substances: hypotheses and reality (a review). *Eurasian Soil Sci.* 54(12). 1826-1854. Doi: <https://doi.org/10.1134/S1064229321120164>
  - [17] Yuan, L., Yan, M., Huang, Z., He, K., Zeng, G., Chen, A., Hu, L., Li, H., Peng, M., Huang, T. and Chen, G. 2019. Influences of pH and metal ions on the interactions of oxytetracycline onto nano-hydroxyapatite and their co-adsorption behavior in aqueous solution. *J. Colloid Interface Sci.* 541. 101-113. Doi: <https://doi.org/10.1016/j.jcis.2019.01.078>
  - [18] Basuki, R., Apriliyanto, Y.B., Stiawan, E., Pradipta, A.R., Rusdianto, B., & Putra, B.R. 2025. Magnetic hybrid chitin-horse manure humic acid for optimized Cd(II) and Pb(II) adsorption from aquatic environment. *Case Stud. Chem. Environ. Eng.* 11. 101138. Doi: <https://doi.org/10.1016/j.csee.2025.101138>
  - [19] Krisbiantoro, P.A., Santosa, S.J., & Kunarti, E.S. 2017. Synthesis of fulvic acid-coated magnetite (Fe<sub>3</sub>O<sub>4</sub>-FA) and its application for the reductive adsorption of [AuCl<sub>4</sub>]<sup>-</sup>. *Indones. J. Chem.* 17(3). 453-460. Doi: <http://dx.doi.org/10.22146/iic.24828>
  - [20] Elsayed, S.A., El-Sayed, I.E., & Tony, M.A. 2022. Impregnated chitin biopolymer with magnetic nanoparticles to immobilize dye from aqueous media as a simple, rapid and efficient composite photocatalyst. *Appl. Water Sci.* 12(11). 252. Doi: <https://doi.org/10.1007/s13201-022-01776-3>
  - [21] Samoilova, N.A. and Krayukhina, M.A. 2020. Chitin-based magnetic composite for the removal of contaminating substances from aqueous media. *Russ. Chem. Bull.* 69(6). 1157-1164. Doi: <https://doi.org/10.1007/s11172-020-2883-7>
  - [22] Salam, M.A. 2017. Preparation and characterization of chitin/magnetite/multiwalled carbon nanotubes magnetic nanocomposite for toxic hexavalent chromium removal from solution. *J. Mol. Liq.* 233. 197-202. Doi: <https://doi.org/10.1016/j.molliq.2017.03.023>
  - [23] Stevenson F.J. 1994. *Humus Chemistry: Genesis, Composition, Reaction*, 2nd edition. John Wiley & Sons: New York.
  - [24] Gunzler, H. and Gremlich, H.U., 2002. *Qualitative spectral interpretation. IR spectroscopy: An introduction*. 171-274. Wiley-VCH: Weinheim, Germany.
  - [25] Chander, S., Yadav, S., Sharma, H.R. and Gupta, A. 2024. Sequestration of Cd(II) utilizing biowaste-fabricated recyclable mesoporous magnetite (Fe<sub>3</sub>O<sub>4</sub>) nano-adsorbent: Process optimization, thermodynamic investigation, simulation modeling, and feasibility for electroplating effluent. *J. Alloys Compd.* 986. 174088. Doi: <https://doi.org/10.1016/j.jallcom.2024.174088>
  - [26] Zarghani, M. & Akhlaghinia, B. 2016. Magnetically separable chitin as an eco-friendly nanocatalyst with high efficiency for green synthesis of 5-substituted-1H-tetrazoles under solvent-free conditions. *RSC Adv.* 6(38). 31850-31860. <https://doi.org/10.1039/C6RA07252F>
  - [27] Jiang, Y., Cai, D., Liu, Q., Shi, Q., Wang. 2023. Adsorption properties and mechanism of Suaeda biochar and modified materials for tetracycline. *Environ. Res.* 235. 116549. Doi: <https://doi.org/10.1016/j.envres.2023.116549>
  - [28] Kusuma, A.K.K.W., Harjito, H., & Jumaeri, J. 2018. Perbandingan massa Ca(NO<sub>3</sub>)<sub>2</sub> dengan SBA-15 terhadap kebasaan katalis reaksi gliserolis. *Indonesian Journal of Chemical Science*. 7(2). 175-181.
  - [29] Pylypchuk, I.V., Kolodyńska, D., Kozioł, M., & Gorbyk, P.P. 2016. Gd-DTPA adsorption on chitosan/magnetite nanocomposites. *Nanoscale Res. Lett.* 11. 1-10. Doi: <https://doi.org/10.1186/s11671-016-1363-3>
  - [30] Serafin, J., & Dziejarski, B. 2023. Application of isotherms models and error functions in activated carbon CO<sub>2</sub> sorption processes. *Micropor. Mesopor. Mat.* 354. 112513. Doi: <https://doi.org/10.1016/j.micromeso.2023.112513>
  - [31] Turlapati, B.K. Prusty, S.K. Pal, E. Raja. 2023. Examining supercritical methane adsorption on nanoporous shales using constant and varying adsorbed phase density approaches. *Energy Fuels*. 37(3). 2078-2090. Doi: <https://doi.org/10.1021/acs.energyfuels.2c03922>
  - [32] Shoaib, A.G., Ragab, S., El Sikaily, A., Yilmaz, M., & El Nemr, A. 2023. Thermodynamic, kinetic, and isotherm studies of Direct Blue 86 dye absorption by cellulose hydrogel. *Scientific Reports*. 13(1). 5910. Doi: <https://doi.org/10.1038/s41598-023-33078-2>
  - [33] Charpentier, T.V., Neville, A., Lanigan, J.L., Barker, R., Smith, M.J. and Richardson, T. 2016. Preparation of magnetic carboxymethylchitosan nanoparticles for adsorption of heavy metal ions. *ACS Omega*. 1(1). 77-83. Doi: <https://doi.org/10.1021/acsomega.6b00035>
  - [34] Karimi, A.R., Fateh, S., Bayat, F. & Abdollahi, M. 2025. Design and characterization of tunable chitosan hydrogels cross-linked with epichlorohydrin through amide bond formation modified with multi-walled carbon nanotubes for adsorption of aflatoxin B1 from aqueous solutions. *J. Macromol. Sci., A*. 62(3). 263-273. Doi: <https://doi.org/10.1080/10601325.2025.2467050>
  - [35] Abdus-Salam, N. & Adekola, S.K. 2018. Adsorption studies of zinc (II) on magnetite, baobab (*Adansonia digitata*) and magnetite-baobab composite. *Appl. Water Sci.* 8(8). 222. Doi: <https://doi.org/10.1007/s13201-018-0867-7>
  - [36] Zhang, N., Reguay, F., Praneeth, S., & Samah, A. K. 2023. A novel green synthesized magnetic biochar from white tea residue for the removal of Pb(II) and Cd(II) from aqueous solution: Regeneration and sorption mechanism. *Environ. Pollut.* 330. 121806. Doi: <https://doi.org/10.1016/j.envpol.2023.121806>